SSRG International Journal of Electrical and Electronics Engineering
ISSN: 2348 – 8379 / https://doi.org/10.14445/23488379/IJEEE-V8I4P107

Volume 8 Issue 4, 36-40, April 2021

Original Article

Inter channel Interference in While box Model of Twin Rotor MIMO System

Huong T.M. Nguyen[1]

[1] *Thai Nguyen University of Technology, Thai Nguyen city, Viet Nam*

Received Date: 03 April 2021
Revised Date: 10 May 2021
Accepted date: 11 May 2021

Abstract *- In model predictive control, building the correct model and solving the optimization problem are two jobs that always require a lot of time and effort. These are also two issues that many scientists are interested in studying when applying model-driven reporting control to certain objects. With a TRMS object, we can build a white box model, a gray box model, or a black-box model. Some authors have built the TRMS model published in [2], [3], [4], [5]. We have studied the optimal problem-solving methods in model predictive control in articles [6], [7], [8]. In this article, the author builds a white-box model of the TRMS object according to the Newton method. Studying the effects of the interchannel effects of the white box model TRMS and evaluation on the ability to apply that model in the simulation and control object.*

Keywords - *While box model, Model predictive control, Yaw angle, Pitch angle, Interchannel Interference, Twin rotor MIMO system (TRMS).*

I. INTRODUCTION

The TRMS is a laboratory set-up designed by Feedback Instrument Ltd [1] and is a suitable test platform for the assessment and implementation of advanced control techniques. The system is connected to a computer through a fast interface to transfer Control signals to the actuators and receive the corresponding feedback signals from the sensors. Moreover, the real-time workshop toolbox of Matlab/Simulink provides an opportunity for the designer to facilitate the controller design procedure Using advanced control toolboxes and other useful built-in functions. The system possesses two propellers perpendicular to each other, one for vertical movement and the other for horizontal motion. However, each one of them significantly affects the motion of the other.

Therefore, the more accurate the TRMS model building, the higher the quality of control in general and predictive control in particular.

II. THE MATHEMATICAL MODEL OF THE TRMS

Considering the TRMS was given in Fig. 1, the physical model as follows:

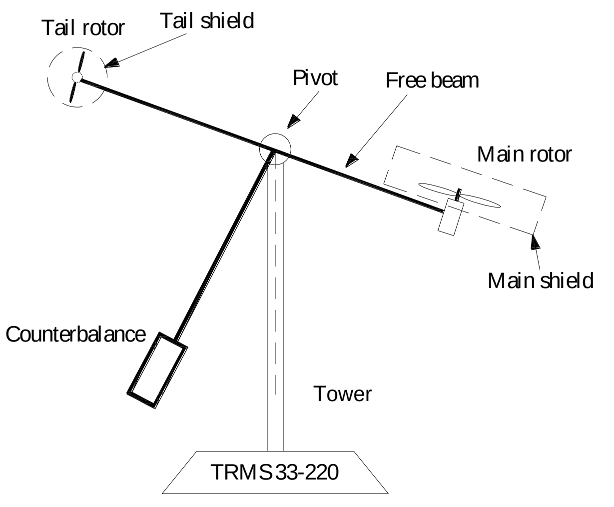

Fig. 1 The TRMS

A. Direct Current Motors

TRMS has two permanent magnet excitation Direct Current Motors, one to drive the main impeller and one to drive the tail rotor. These two engines are the same, but the mechanical loads are different. The circuit diagram of them is shown in Fig. 2, the mathematical equations from (1) to (5) controlling the main motor and the tail motor [2].

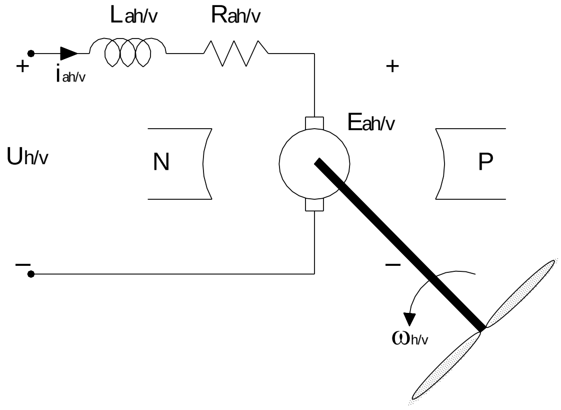

Fig. 2 Circuit diagram of the DC motor

$$U_{h/v} = E_{ah/v} + R_{ah/v} i_{ah/v} + L_{ah/v} \frac{di_{ah/v}}{dt} \quad (1)$$

$$E_{ah/v} = k_{ah/v} \varphi_{h/v} \omega_{h/v} \quad (2)$$

$$M_{eh/v} = M_{Lh/v} + J_{tr/mr} \frac{d\omega_{h/v}}{dt} + B_{tr/mr} \omega_{h/v} \quad (3)$$

$$M_{eh/v} = k_{ah/v} \varphi_{h/v} i_{ah/v} \quad (4)$$

$$M_{Lh/v} = k_{th/v} sign(\omega_{h/v}) \omega_{h/v}^2 \quad (5)$$

Where:

$E_{ah/v}$: Electromotive force of the tail/main motor (V)
$R_{ah/v}$: Armature resistance of the tail/main motor (Ω)
$L_{ah/v}$: Armature inductance of the tail/ main motor (H)
$i_{ah/v}$: Armature current of the tail/ main motor (A)
$k_{ah/v}$: Constant (Nm/AWb)

$\varphi_{h/v}$: Magnetic flux of the tail/main motor (Wb)

$M_{eh/v}$: Electromagnetic torque of the tail/main motor (Nm)
$M_{lh/v}$: Load torque of the tail/main motor (Nm)
$J_{tr/mr}$: Moment of inertia of the tail/main DC motor (kg m^2/s)

K_{tvp}, k_{tvn}: Constants (Nms^2/rad^2)

$\omega_{h/v}$: Rotational velocity of the tail/main rotor (*rad/s*)

$U_{h/v}$: Input voltage signal of the tail/main motor (*V*)

B. The Newtonian-based Modelling of the TRMS

Modem methods of design and adaptation of real-time controllers Require high-quality mathematical plant models. For high order nonlinear cross-coupled systems such as the TRMS in Fig. 3, classical modeling methods based on Lagrange's equations or the Newton approximation are often used.

The input signals of TRMS in Fig. 3 are U_v and U_h (input voltage of the main motor and tail motor), the output is α_v and α_h (pitch angle and yaw angle). This inter-channel effect is also present in aircraft and most MIMO systems, which is why the control model and problem become a challenge for these systems.

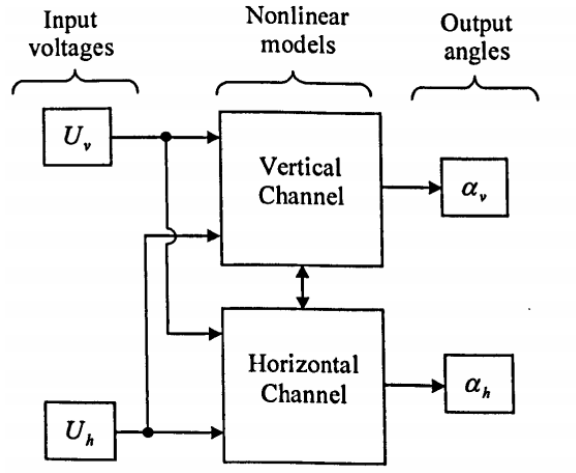

Fig. 3 Coupled MIMO model of TRMS

The control input signal is the voltage applied to the DC motor. When the voltage magnitude changes, the angular velocity of the impeller changes, leading to the force acting on the swingarm changes causing the swingarm. Move to a new position, i.e., change the pitch angle and yaw angle. According to the Law of conservation of momentum, when the rotor rotates to produce dynamic torque, the body of the TRMS generates a compensating torque for the system to balance. This is the cause of the interchannel effect in the swingarm's movement on both planes (vertical and horizontal channels).

Use Newton's approximation method to model the rest of the system mathematically, as shown in equations (6) to (13) [2]. (Fig. 4).

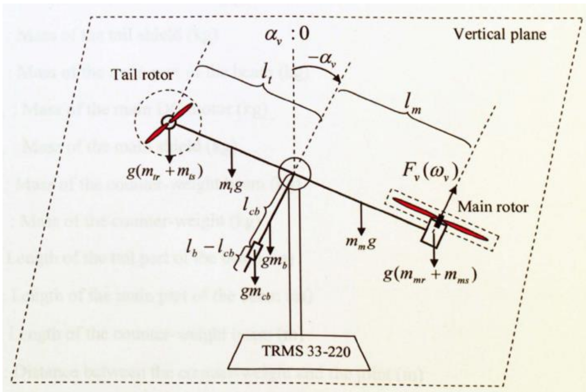

Fig. 4 Gravity and repulsion in the vertical projection plane

In equation (6), the first term represents the moment of the main rotor; the second term is the moment of friction; the third term represents the moment of gravity; the fourth term denotes the moment of centrifugal force during the rotation of the lever arm on the horizontal plane, and the 5th term is the torque of the gyroscope effect. The second term in equation (8) denotes the effect of the tail rotor speed on the swingarm's motion on the vertical plane.

$$\frac{dS_v}{dt}=\frac{l_m F_v(\omega_v)-M_{fric,v}+g[(\mathrm{A}-\mathrm{B})\cos\alpha_v-\sin\alpha_v]}{J_v}$$
$$+\frac{-0.5\Omega_h^2 H\sin 2\alpha_v+k_g F_v(\omega_v)\Omega_h\cos\alpha_v}{J_v} \qquad (6)$$

Where

$$A=\left(\frac{m_t}{2}+m_{tr}+m_{ts}\right)l_t;\; B=\left(\frac{m_m}{2}+m_{mr}+m_{ms}\right)l_m$$

$$C=\left(\frac{m_b}{2}l_b+m_{cb}l_{cb}\right)$$

$$H=Al_t+Bl_m+\frac{m_b}{2}l_b^2+m_{cb}l_{cb}^2$$

$$F_v(\omega_v)=\begin{cases}k_{fvp}.|\omega_v|.\omega_v & \omega_v\ge 0\\ k_{fvn}.|\omega_v|.\omega_v & \omega_v<0\end{cases} \qquad (7)$$

$$\Omega_v=S_v+\frac{k_t\omega_h}{J_v} \qquad (8)$$

$$\frac{d\omega_v}{dt}=\Omega_v \qquad (9)$$

In equation (10), the first term represents the moment of the tail rotor (impeller); the second term is the moment of friction; and the last term denotes the moment caused by the gyroscope effect, which is a completely nonlinear quantity and can be obtained by measuring it point by point. The second term in equation (12) denotes the effect of the main rotor (impeller) speed on the swingarm's motion on the horizontal plane.

$$\frac{dS_h}{dt}=\frac{l_t F_h(\omega_h)\cos\alpha_v-M_{fric,h}-M_{cable}(\alpha_h)}{D\cos^2\alpha_v+E\sin^2\alpha_v+F} \qquad (10)$$

Where:

$$D=\left(\frac{m_m}{3}+m_{mr}+m_{ms}\right)l_m^2+\left(\frac{m_t}{3}+m_{tr}+m_{ts}\right)l_t^2;$$

$$E=\frac{m_b}{3}l_b^2+m_{cb}l_{cb}^2;\; F=m_{ms}r_{ms}^2+\frac{m_{ts}}{2}r_{ts}^2$$

$$F_h(\omega_h)=\begin{cases}k_{fhp}.|\omega_h|.\omega_h & \omega_h\ge 0\\ k_{fhn}.|\omega_h|.\omega_h & \omega_h<0\end{cases} \qquad (11)$$

$$\Omega_h=S_h+\frac{k_m\omega_v\cos\alpha_v}{D\cos^2\alpha_v+E\sin^2\alpha_v+F} \qquad (12)$$

$$\frac{d\alpha_h}{dt}=\Omega_h \qquad (13)$$

Where:

g: Gravitational acceleration (m/s^2)
m_t: Mass of the tail part of the beam (kg)
m_{tr}: Mass of the tail DC motor (kg)
m_{ts}: Mass of the tail shield (kg)
m_m: Mass of the main part of the beam (kg)
m_{mr}: Mass of the main DC motor (kg)
m_{ms}: Mass of the main shield (kg)
m_b: Mass of the counter-weight beam (kg)
m_{cb}: Mass of the counter-weight (kg)
l_t: Length of the tail part of the beam (m)
l_m: Length of the main part of the beam (m)
l_b: Length of the counter-weight beam (m)
l_{cb}: Distance between the counter-weight and the joint (m)
α_v: Pitch angle of the TRMS beam (*rad*)
α_h : Yaw angle of the TRMS beam (*rad*)
ω_v: Rotational velocity of the main rotor(*rad/s*)
ω_h: Rotational velocity of the tail rotor (*rad/s*)
U_v: Input voltage signal of the main motor (*V*)
U_h: Input voltage signal of the tail motor (*V*)
Ω_v: Angular velocity (pitch velocity) of the TRMS beam (rad/s)
Ω_h: Angular velocity (azimuth velocity) of the TRMS beam (rad/s)
S_v: Angular velocity of the TRMS beam in the vertical plane without the effect of the tail rotor (*rad/s*)
S_h: Angular velocity of the TRMS beam in the horizontal plane without the effect Of the vertical channel (rad/s).

III. SIMULATION RESULTS

The one-degree and two-degree TRMS object model on Matlab / Simulink is shown in Fig. 5 and Fig. 6.

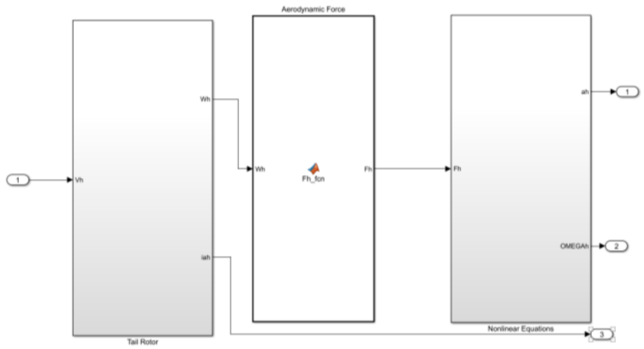

Fig. 5 TRMS block diagram of a degree of freedom vertically

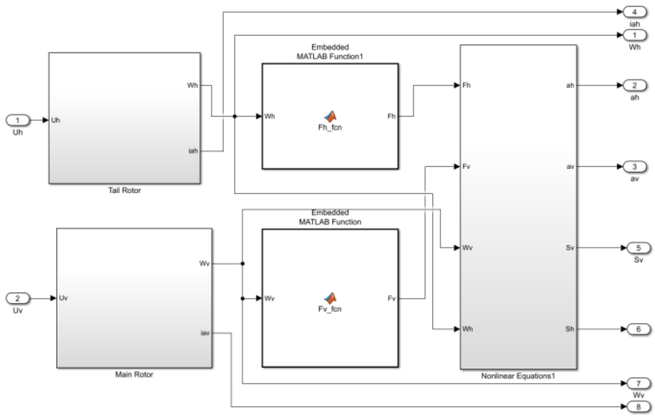

Fig. 6 Complete block diagram simulation of TRMS two degrees of freedom

The internal structure of the tail engine block and the main engine is shown in Fig. 7, Fig. 8.

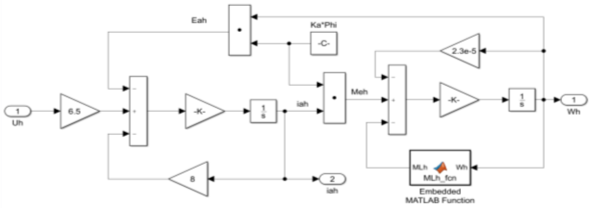

Fig. 7 The internal structure of the tail rotor

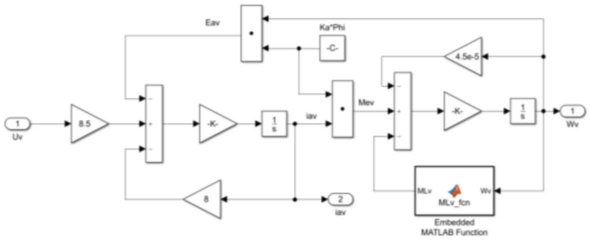

Fig. 8 The internal structure of the main rotor

The internal structure of the nonlinear functions simulates two degrees of freedom TRMS is shown in Fig. 9.

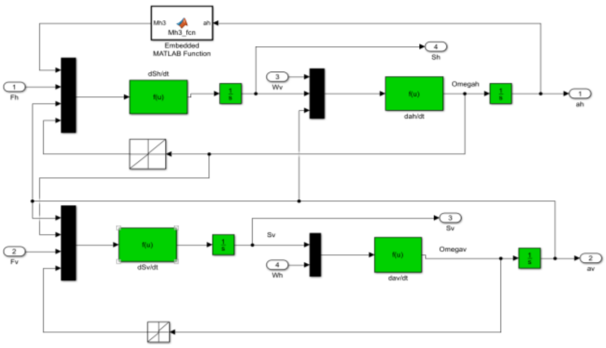

Fig. 9 The internal structure of the nonlinear functions simulates two degrees of freedom TRMS

Fig. 10 to 12 are 1DOF models of the yaw angle, and Fig. 13 to 15 are 1DOF models of pitch angle when the signal is set sine, step, and square pulse, respectively.

Fig. 10 The yaw angle of the TRMS model when the set signal is a sine

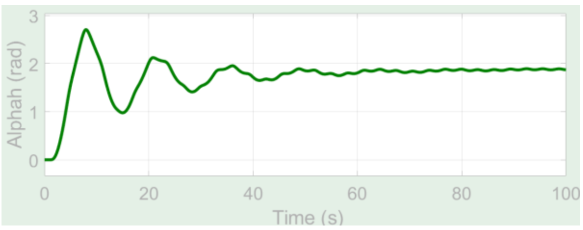

Fig. 11 The yaw angle of the TRMS model when the set signal is step

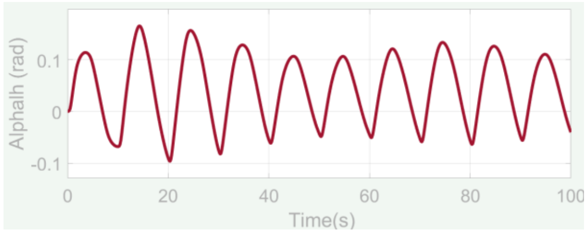

Fig. 12 The yaw angle of the TRMS model when the set signal is a square pulse

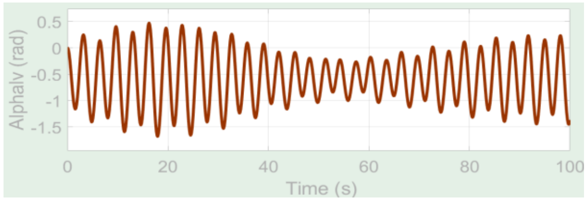

Fig. 13 The pitch angle of the TRMS model when the set signal is a sine

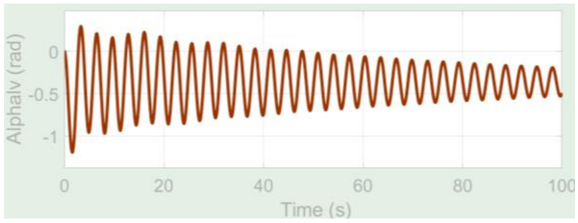

Fig. 14 The pitch angle of the TRMS model when the set signal is step

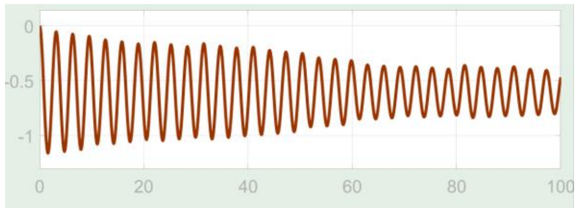

Fig. 15 The pitch angle of the TRMS model when the set signal is a square pulse

Fig. 16 to 21 are 2DOF model of TRMS that clearly shows the interchannel effect between the vertical and horizontal channels when the signal is set as sine, step and square pulse, respectively.

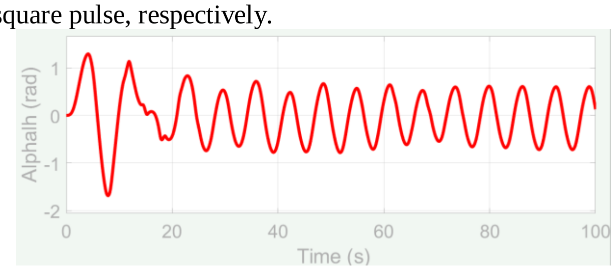

Fig. 16 The yaw angle of the TRMS model when the set signal is sine and affected by pitch angle

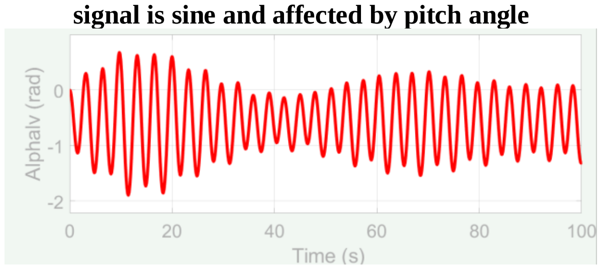

Fig. 17 The pitch angle of the TRMS model when the set signal is sine and affected by yaw angle

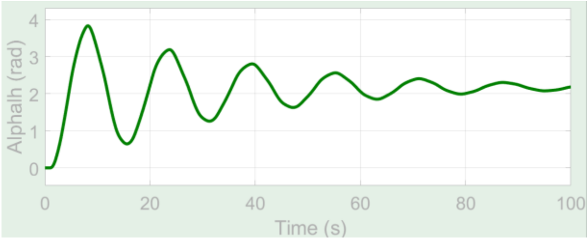

Fig. 18 The yaw angle of the TRMS model when the set signal is step and affected by pitch angle

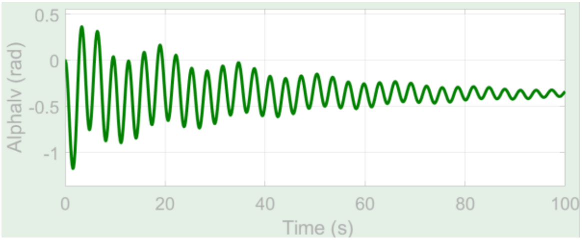

Fig. 19 The pitch angle of the TRMS model when the set signal is step and affected by yaw angle

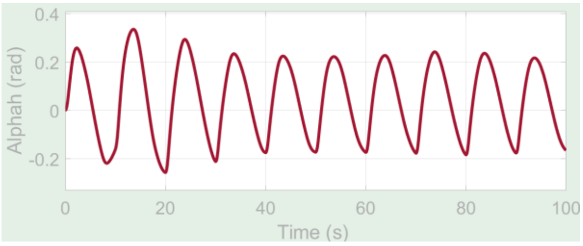

Fig. 20 The yaw angle of the TRMS model when the set signal is the square pulse and affected by pitch angle

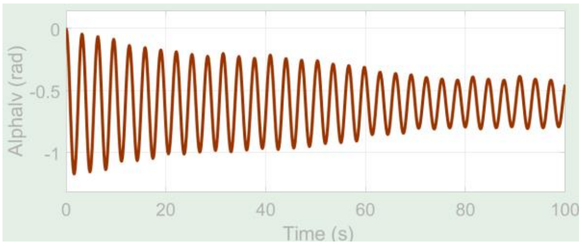

Fig. 21 The pitch angle of the TRMS model when the set signal is the square pulse and affected by yaw angle

Comments: The simulation results for a vertical and horizontal one degree of freedom model show that when the signal applied to the model is changed to a sine, step, square pulse, the first response is changed. The output model differs from the two degrees of freedom model when the set signal is also sine, step, square pulse. This proves that there is a very clear inter-channel effect woven between the vertical and horizontal channels. Specifically: With the same signal set sine, step, a square pulse, the output response of the reversal angle respectively in Fig. 10, Fig. 11, Fig. 12 without inter-channel interchange and Fig. 16, Fig. 18. Fig. 20 shows the steering reversal angle when inter-channel effects are applied. Similarly, with the same signal set sine, step, square pulse respectively, the output response of the pitch angle is Fig. 13, Fig. 14, Fig. 15 without interchannel interference, and Fig. 17, Fig. 19 Fig. 21 shows the yaw angle when inter-channel effects are applied.

Through these simulation results also shows that the pitch angle and the yaw angle have a quite pronounced effect of intermingling. However, the degree of channel alternation of the pitch angle has a greater influence on the yaw angle and vice versa, and the yaw angle affects the channel alternating less the pitch angle. In the process of controlling, solving this problem is still a big challenge.

V. CONCLUSION

Constructing a mathematical model of the TRMS system according to the white box model using Newton's approximation method through Matlab's simulation clearly shows the inter channel effect of the yaw angle and the pitch angle in the horizontal plane and the vertical plane of this system. In the next expected research, the author will build a black-box model through a genetic algorithm or neural network identification to exploit, apply modern control methods to control TRMS objects.

VI. ACKNOWLEDGEMENTS

The work described in this paper was supported by the Thai Nguyen University of Technology (http://www.tnut.edu.vn/).

VII. REFERENCES

[1] Twin Rotor MIMO System 33-220 User Manual, 1998 (Feedback Instruments Limited, Crowborough, UK).

[2] A. Rahideh, M.H. Shaheed, Mathematical dynamic modeling of a twin-rotor multiple inputs–multiple output system, Proceedings of the IMechE, Part I. Journal of Systems and Control Engineering 221 (2007) 89–101.

[3] Ahmad, S. M., Shaheed, M. H., Chipperfield, A. J., and Tokhi, M. O. Nonlinear modeling of a twin-rotor MIMO system using radial basis function networks. IEEE National Aerospace and Electronics Conference, (2000) 313–320.

[4] Ahmad, S. M., Chipperfield, A. J., and Tokhi, M. O. Dynamic modeling and optimal control of a twin-rotor MIMO system. IEEE National Aerospace and Electronics Conference, 2000, pp. 391–398.

[5] Shaheed, M. H. Performance analysis of 4 types of conjugate gradient algorithm in the nonlinear dynamic modeling of a TRMS using feedforward neural networks. IEEE International Conference on Systems, man and cybernetics, (2004) 5985–5990.

[6] Huong T.M. Nguyen, Thai. Mai.T, Anh. Do. T.T, Lai Lai K. Stabilization for Twin Rotor MIMO System based on BellMan's Dynamic Programming Method, Journal of Science and Technology of Thai Nguyen University,128(14) (2014) 161-165.

[7] Huong. Nguyen. T.M, Thai. Mai.T, Chinh. Nguyen. H, Dung. Tran.T and Lai. Lai. K, Model Predictive Control for Twin Rotor MIMO system, The University of Da Nang Journal of Science and Technology, 12[85] (2014) 39 – 42.

[8] Huong T.M. Nguyen, Thai Mai T., Lai Lai K., Model Predictive Control to get Desired Output with Infinite Predictive Horizon for Bilinear Continuous Systems, International Journal of Mechanical Engineering and Robotics Research, 4(4) (2015) 299 - 303.